JOURNAL OF Applied Polymer SCIENCE

Controlled synthesis of magnetic block copolymers for anti-microbial purpose

Hongjian Zhao
School of Materials Science & Engineering, Tianjin University, Tianjin, 300072, China
Correspondence to: H. Zhao (E-mail: hjzhao@tju.edu.cn)

ABSTRACT: Magnetic block copolymers (PNIFe-*b*-PNC) with a well-defined and controllable structure were synthesized via ring opening metathesis polymerization (ROMP) and post modification with ferric trichloride hexahydrate ($FeCl_3 \cdot 6H_2O$). The magnetic properties, surface morphology and antimicrobial activities for Gram-positive bacteria and Gram-negative bacteria of magnetic copolymers were studied. All of the magnetic copolymers were characterized of paramagnetic properties. The susceptibilities were affected by the content of imidazolium $FeCl_4^-$ and the degree of polymerization of copolymers. The maximum magnetic susceptibility was 20.96×10^{-6} emu/g ($PNIFe_{150}$-*b*-PNC_{50}). The magnetic copolymers showed high thermal stability and start to decompose at 350 °C. The magnetic copolymers showed higher and broader-spectrum antimicrobial activity, which leads to the well-defined magnetic polymers materials having the potential applications in wide fields such as antimicrobial fi... J. Appl. Polym. Sci. **2017**, *134*, 44598.

KEYWORDS: applications; copolymers; ionic liquids; ring-opening polymerization

Received 7 May 2016; accepted 18 October 2016
DOI: 10.1002/app.44598

INTRODUCTION

Magnetic polymer materials have been paid much attention due to their extensive applications in magnetic separation,[1] magnetic resonance imaging,[2] catalyst for reaction,[3] and drug delivery.[4] However, the magnetic polymers were mainly prepared via hybridization of polymers with inorganic magnetic nanoparticles via physical/chemical interactions[5,6] and the preparation for polymers with magnetic properties themselves remains a great challenge. In 1980s, the first organic ferromagnet was obtained via the polymerization of side-chain radical containing biacetylene and the resultant polymers had magnetic properties which were from the high-spin polyradicals since that selected conjugated hydrocarbon polyradicals had strong ferromagnetic couplings.[8] With the development of polymer chemistry, magnetic polymers complexing with transition metal or paramagnetic ions were reported[8] and have attracted increasing attention because of their facile design and synthesis compared with the conjugated polyradicals.

In 2004, Hyashi and Hamaguchi discovered a novel paramagnetic ionic liquid containing tetrahalogen iron(III) anion, such as tetrachloroferrate ($FeCl_4$), which were prepared by mixing quaternized ammonium salt with iron(III) halide.[9] This paramagnetic ionic liquid has unique magnetic response which has potential in magnetic control and separation.[10,11] Later, Döbbelin[12] synthesized paramagnetic poly(ionic liquid) containing $FeCl_4$ and tetrabromoferrate ($FeBr_4$) and the poly(-ionic liquid)s were used as a reusable catalyst in Friedel–Crafts alkylation. The paramagnetic poly(ionic liquid) can be easily separated and reused after the reaction, which made them interesting for green chemistry processes. Recently, magnetic block polymers have been prepared using as thermosetting materials and fluorescent materials via post-modification of pyridine or imidzole with $FeCl_4$.[13,14] It is worth noting that all the magnetic polymers were prepared through quaternization of precursor polymer and modification with $FeCl_3 \cdot 6H_2O$. However, the quaternization for polymers were difficult and the magnetic anion $FeCl_4^-$ was not uniform in every repeated unite, which limited the controllability and magnetic properties of resultant polymers. Living ring-opening metathesis polymerization (ROMP) was widely used in developing a variety of well-defined polymers with controlled molecular weight and various architectures. Comparing with the other living polymerization, ROMP had a mild condition and simple procedure. Above all, there was a high efficiency conversion for ROMP polymerization.[15–17] The novel paramagnetic polymers synthesized via ROMP would have perfect structure and potential applications.

As known, the structure of quaternary ammonium salts has antimicrobial performance and it is the most popular antimicrobial material owing to its simple fabrication process and low cost, though it has relatively lower antimicrobial efficacy

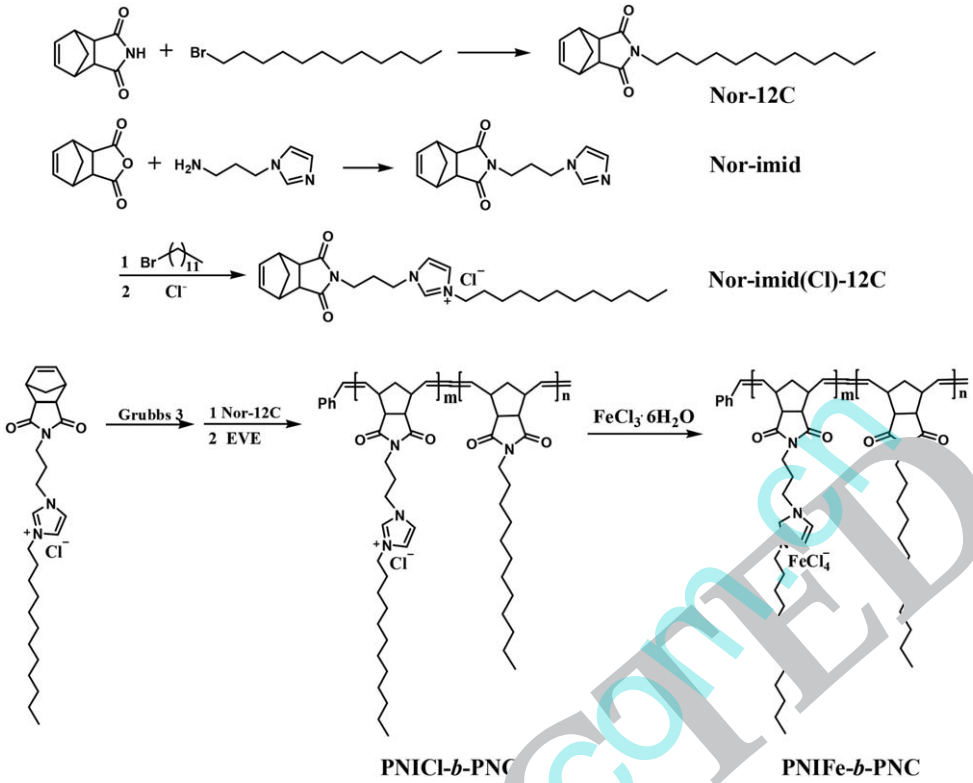

Scheme 1. Synthesis of PNIFe-b-PNC magnetic block copolymers.

compared with polymeric N-halamines and antimicrobial peptides.[18–20] Bringing in magnetism seems promising to obtain multifunctional materials. From the aspect of application, block copolymers have been studied intensively, concerning the possible self-assembly in both bulk and selective solution.[21–26] The self-assembled structures therefore have potential applications in antimicrobial materials.[27] An added benefit of block copolymers is that their chemical composition can be altered to obtain different mechanical properties and morphology without affecting the basic properties of the individual domains.[28,29] In the previous research, a series of polycationic magnetic polymers based on polyethyleneimine (PNIFe-b-PEI) were synthesized via quaternization and post-polymerization with $FeCl_3 \cdot 6H_2O$, which indicated that the polymers could be film due to the nature of polymer electrolyte. In order to obtain magnetic polymer films, a series of block copolymers containing alkyl substituted norbornene derivative and imidazolium chloride based norbornene derivative were prepared via ROMP and post-modification in this research. The flexible alkyl side-chain was not only improving compliance of copolymer, but also contributing for self-assembling due to their hydrophilicity different from imidazolium tetrachloroferrate ($FeCl_4$).[31,32] It was hypothesized that tailoring imidazolium $FeCl_4$ block with controlled chain length via ROMP polymerization would provide a unique method to investigate the effects of magnetic blocks on the magnetic properties and the surface morphology of copolymer films. Considering for the structure–antimicrobial relationships, the antimicrobial activity of the magnetic block copolymer films was studied by using Gram-positive bacteria, *Bacillus subtilis* (*B. subtilis*) and Gram-negative bacteria, *Escherichia coli* (*E. coli*), respectively.

EXPERIMENTAL

Materials

Cis-5-norbornene-exo-2,3-dicarboxylic anhydride (98%, Energy Chemical), N-(3-aminopropyl)imdazole (98%, HEOWNS), 5-norbonene-2,3-dicarboximide (98%, Energy Chemical), 1-bromododecane (99%, HEOWNS), ion exchange resin (Amberlite IRA-400(Cl), Alfa Aesar), $FeCl_3 \cdot 6H_2O$ (99%, Tianjin Shuangchuan Chemical Reagent Factory), Grubbs catalyst 2rd (Sigma-Aldrich), and all the other chemicals were commercially available and used directly unless addressed.

Characterizations

^{1}H-nuclear magnetic resonance (^{1}H NMR) spectra were conducted on a 500 MHz Bruker Avance III NMR spectrometer and all of the chemical shifts were reported in ppm. Raman measurements were carried out on a DXR Microscope at a wavelength of 780 nm. Magnetic measurements were conducted on a Superconducting Quantum Interference Device (SQUID) Quantum Design PPMS-9 magnetometer at 300 K in the magnetic field range of −10,000 to 10,000 Oe. The surface morphology of the magnetic copolymer films were characterized by atomic force microscopy (AFM, CSPM5500A, Being Nano-Instruments, Ltd., China) and scanning electron microscopy (SEM, Hitachi S-4800, Japan). AFM was measured in tapping mode and samples were imaged at 3 μm ×3 μm magnifications using a nanosensor silicon tip. Thermogravimetric analysis (TGA) was conducted on a Pyris 1 TGA (PerkinElmer System),

Table I. The Feeding Ratios for ROMP Polymerization and Preparing Block Polymers $PNIFe_m$-*b*-PNC_n

m:n[a]	50:50	100:50	150:50	150:100	150:150
Nor-imid(Cl)−12C(mmol)	2	4	6	3	3
Nor-12C (mmol)	2	2	2	2	3
Grubbs 3rd (mmol)	0.04	0.04	0.04	0.02	0.02
$FeCl_3 \cdot 6H_2O$ (mmol)	2	4	6	3	3

[a] Feeding ratios for copolymerization of theoretical design, m is for Nor-imid(Cl)−12-C and n is for Nor-12C.

ramping from 25 °C to 1000 °C at a rate of 10 °C/min under the protection of nitrogen.

Synthesis of Norbornene Derivative Based on Imidazolium Chloride Nor-Imid(Cl)-12C

Nor-imid(Cl)-12C was prepared following the procedure shown in Scheme 1. Equivalent Cis-5-norbornene-exo-2,3-dicarboxylic anhydride (0.05 mol, 8.8005 g) and N-(3-aminopropyl)imdazole (0.05 mol, 6.3865 g) were dissolved in CH_2Cl_2 and stirred under room temperature for 4 h. Then the solvent was removed by rotary evaporator. The mixture left was reacted under 120 °C for 5 h and dried in the vacuum to obtain compound Nor-imid. ^{1}HNMR (500 MHz, $CDCl_3$, ppm), δ = 7.60(s, 1H, —CH_2(CH)NC<u>H</u>=N—), 7.08(s, 1H, —CH_2(CH)NC<u>H</u>=CHN—), 6.96(s, 1H, —CH_2(CH)NCH=C<u>H</u>N—), 6.27(s, 2H, —CHC<u>H</u>=C<u>H</u>CH—), 3.98(t, 2H, J = 7, —N<u>C</u>$H_2CH_2CH_2$N—), 3.53(t, 2H, J = 10, —$NCH_2CH_2CH_2$N—), 3.27(s, 2H, —C<u>H</u>(CH)C=O—), 2.67(s, 2H, —CHCH=CHC<u>H</u>(CH_2)CH—), 2.11–2.06(m, 2H, —$NCH_2CH_2CH_2$N—), 1.52(d, 2H, J = 5, —CH=CHCH(CH)C<u>H_2</u>CH—), 1.16(d, 2H, J = 5, —CH=CHCH(CH)C<u>H_2</u>CH—).

Nor-imid (20 mmol, 5.4226 g) and double equivalent 1-bromododecane (10 mmol, 2.5000 g) were dissolved in acetone and refluxed under 60 °C for 24 h. The solution was concentrated with rotary evaporator and precipitated in ethyl ether to remove excess bromine and hydrocarbons. The precipitation was dried in the vacuum to obtain the pure imidazolium bromide Nor-imid(Br)−12C. Nor-imid(Br)−12C was dissolved in methane and ion exchange resin of chloride (10 g) was washed with methane before adding the solution of the product. The solution was stirred under room temperature for 8 h. Then ion exchange resin was filtered and the solvent was removed through rotary evaporator. The crude product was dried until constant weight to obtained imidazolium chloride Nor-imid(Cl)-12C. ^{1}HNMR (500 MHz, $CDCl_3$, ppm), δ = 10.52(s, 1H, —CH_2(CH)NC<u>H</u>=N—), 7.64(s, 1H, —CH_2(CH)NC<u>H</u>=CHN—), 7.26(s, 1H, —CH_2(CH)NCH=C<u>H</u>N—), 6.28(s, 2H, —CHC<u>H</u>=C<u>H</u>CH—), 4.49–4.46(t, 2H, —N^+ <u>CH_2</u>CH_2—), 4.29–4.27(t, 2H, —NCH_2CH_2C<u>H_2</u>N—), 3.52–3.50(t, 2H, —N<u>C</u>$H_2CH_2CH_2$N—), 3.25(s, 2H, —CHC<u>H</u>(CH)C=O—), 2.88(s, 2H, —CHCH=CHC<u>H</u>(CH_2)CH—), 2.29–2.24(m, 2H, —$NCH_2CH_2CH_2$N—), 1.94–1.90(m, 2H, —CH_2<u>CH_2</u>CH_3), 1.52(d, 2H, —CHC<u>H_2</u>CH—), 1.35–1.20(broad, 18H, —N^+ CH_2<u>$(CH_2)_9$</u>CH_2CH_3), 1.15(d, 2H, —CHC<u>H_2</u>CH—), 0.88–0.85(t, 3H, —CH_2<u>CH_3</u>).

Synthesis of Norbornene Derivative Based on Alkyl Group Nor-12C

5-Norbonene-2,3-dicarboximide (25 mmol, 4.1628 g), 1-bromododecane (30 mmol, 7.4700 g) and K_2CO_3 (25 mmol, 3.4500 g) were dissolved in 100 mL DMF and stirred under room temperature for 24 h. Then the solvent was removed through rotary evaporator and the mixture left was extracted with CH_2Cl_2 and H_2O. The organic phase was concentrated and precipitated in petroleum ether for three times to purify the product. The precipitation was dried under vacuum to constant weight to obtain Nor-12C. ^{1}HNMR (500 MHz, $CDCl_3$, ppm), δ = 6.09(s, 2H, —CHCH=CHCH—), 3.38(s, 2H, —CHC<u>H</u>(CH)C=O—), 3.32–3.29(t, 2H, —N<u>C</u>H_2CH_2—), 3.22(s, 2H, —CHCH=CHC<u>H</u>—), 1.72(d, 2H, —CHC<u>H_2</u>CH—), 1.53(d, 2H, —CHC<u>H_2</u>CH—), 1.43–1.37(m, 2H, —NCH_2C<u>H_2CH_2</u>—), 1.30–1.20(broad, 18H, —NCH_2CH_2<u>$(CH_2)_9$</u>—), 0.88–0.86(t, 3H, —CH_2CH_3).

Synthesis of Magnetic Block Copolymers (PNIFe-*b*-PNC)

The magnetic block polymers (PNIFe-*b*-PNC) were prepared via ring-opening metathesis polymerization and modifying the polymers precursor. Here, copolymerizable monomers we chose for polymerization were Nor-imid(Cl)-12C and Nor-12C. Grubbs catalyst 3rd generation used in this research was prepared according to the Ref. 33. Five different feeding ratios were chose and shown in Table I. As shown in Scheme 1, Nor-imid(Cl)-12C and Grubbs 3rd were dissolved in CH_2Cl_2, mixed and stirred under room temperature for 30 minutes. Then the second monomer Nor-12C was dissolved in CH_2Cl_2 and added for copolymerization. Ten minutes later, excess ethyl vinyl ether (EVE) was added into the reaction system of polymerization and stirred for another 30 minutes and then the polymerization solution precipitated in petroleum ether for several times. The precipitation was dried in the vacuum to obtain block copolymers $PNICl_m$-*b*-PNC_n. $PNICl_m$-*b*-PNC_n precursor obtained were reacted with $FeCl_3 \cdot 6H_2O$ in methane as the feeding in Table I. Reaction mixture was stirred under 50 °C for 24 h and then precipitated in ethyl ether. The crude product was dried in the vacuum to obtain pure magnetic block copolymers $PNIFe_m$-*b*-PNC_n.

Assessment of Antimicrobial Properties

The magnetic block copolymer films used for antimicrobial assessment were prepared through spin coating method. The obtained magnetic block copolymers were dissolved in a mixed solvent of acetonitrile and TFT (*v*/*v* = 5/5) to prepare the copolymer solution (30 wt %) and the magnetic copolymer solution

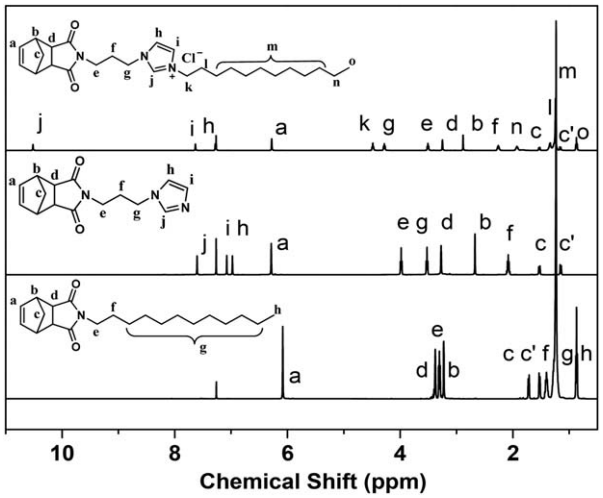

Figure 1. ^{1}HNMR spectra of Nor-12C, Nor-imid, Nor-imid(Cl)−12C in $CDCl_3$.

(200 L) was spin-coated on clean teflon membrane which was fixed on aluminum sheets (2 cm × 2 cm) with the rotating speeds at 600 r/s for 30s firstly and followed 3000 r/s for 50s. The solvent was evaporated at room temperature until the magnetic films were taken shape. The magnetic copolymer films obtained were placed in the condition which was suffused with acetonitrile vapor pressure for movement of polymer chains with a longer time, so as to get a better result of self-assemble. The magnetic copolymer films were taken down from [illegible] and the thicknesses of the obtained magnetic copolymer films were around 0.5 mm. These films were used for the characterization of surface morphology, magnetic properties and antimicrobial activity testing. The antimicrobial property of the magnetic copolymer films was studied with [illegible] agar plating method according to the Refs. 34–37. For these experiments, 200 L of initial bacteria (10^5−10 C[illegible]/mL) was added on the nutrient agar plates and distributed uniformly. The surface of copolymer films contacted with the agar directly in the plates, which were inverted and incubated for 24 h at 37 °C. Then around the magnetic films, inhibition of microbial growth was evaluated visually. If a transparent inhibition zone appeared, "+" was denoted for indicating antimicrobial response. Conversely, if not, "−" was [illegible]

RESULTS AND DISCUSSION

Synthesis of Magnetic Block Polymer (PNIFe$_m$-*b*-PNC$_n$)

The magnetic block polymers have been synthesized through ROMP and post-polymerization. Monomers used for ROMP polymerization were prepared as per the procedure shown in Scheme 1. Equivalent amounts of Cis-5-norbornene-exo-2,3-dicarboxylic anhydride and N-(3-aminopropyl)imdazole were mixed and reacted to obtain pale yellow viscous substance, which was in a different state with both reactants. The product norbornene derivative was prepared using the nucleophilic addition reaction between acid anhydride and amino groups. As shown in Figure 1, a broad peak on behalf of amino group does not exist and this suggests that the amino group has completely reacted. The three peaks at 7.60, 7.08, and 6.96 ppm were all signal and their ratios of integrated areas was 1:1:1, which present "j" "i" "h" in the imidazole ring. A typical signal peak at 6.27 ppm was characterized for double bond "a" in norbornene anhydride. The double peaks at 1.52 ppm and 1.16 ppm was characterized for "c," which resulted from the coupling of two hydrogen. The hydrogen of "b" and "d" were both single peaks at 2.67 and 3.27 ppm. The peak of "d" appears at low field because of the electron-withdrawing effect of the carbonyl group connecting with the carbon atom. The peaks at 3.98 and 3.53 ppm were both triplet due to connecting with methylene (—CH_2—), which represented for "e" and "g" due to the electron effect amino groups was stronger than that of amide group. The hydrogen of "f" was at the presentation quintet at 2.11–2.06 ppm because of both sides connecting to methylenes. By integrating for every peak, the numbers of hydrogen can be drawn with the same proportion of the areas which could indicate that Nor-imid have been successfully prepared.

Nor-imid was quaternized with 1-bromododecane and then reacted with ion exchange resin of chloride. Figure 1 showed the ^{1}HNMR spectrum of the product. Compared with ^{1}HNMR spectrum of Nor-imid, almost every peak shifted downfield because of the formation of quaternary ammonium salts. The peaks for "j" "i" and "h" shifted downfield due to the electron-withdrawing effect of N^+ in the imidazolium. The distance between the hydrogen in norbornene amide and quaternary ammonium salt group was farther and this resulted in no change in the displacement. By integrating every peak, the number of hydrogen can be drawn with the same proportion of the areas and the splitting of every peak matched with their chemical environment in the structure, which could indicate that Nor-imid(Cl)-12C was obtained.

Another monomer norbornadiene alkene derivatives Nor-12C was synthesized through mixing 5-norbonene-2,3-dicarboximide and 1-bromododecane. Figure 1 shows the ^{1}H NMR spectrum of the products. The peaks of "a," "d," and "b" were unimodal and "c" was splitting into two doublets. The hydrogen for "e" and "h" were triplet due to connecting with methylene, and

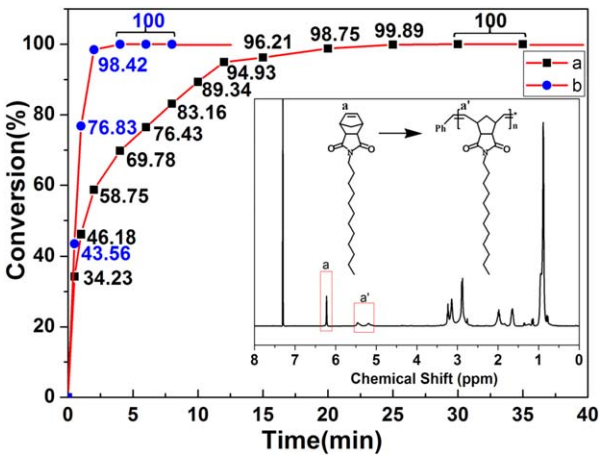

Figure 2. The polymerization conversion of ROMP for Nor-imid(Cl)−12C(a) and Nor-12C(b) versus polymerization time (the inert was the ^{1}HNMR spectrum used for calculating the polymerization conversion). [Color figure can be viewed at wileyonlinelibrary.com]

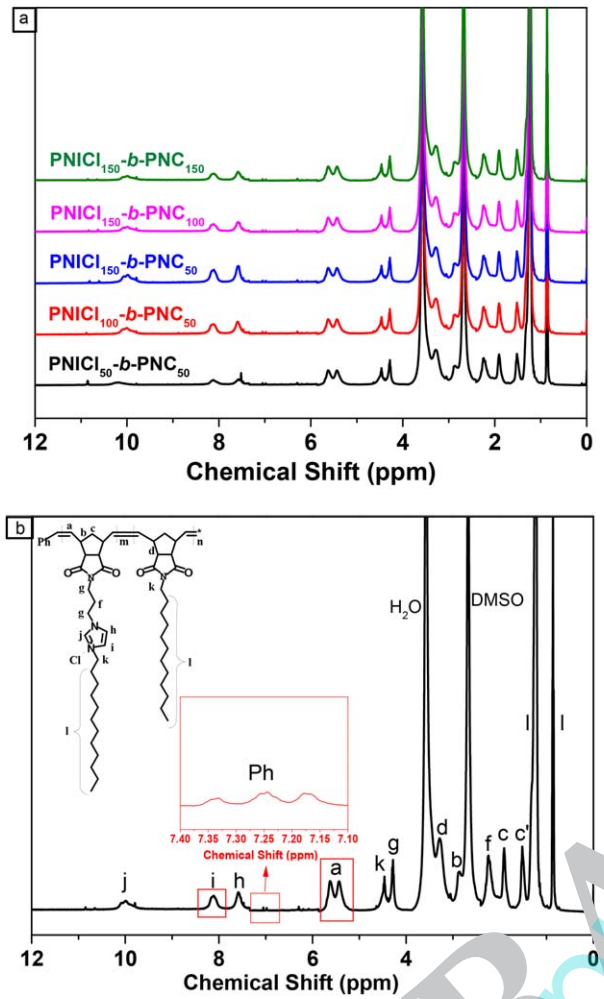

Figure 3. ^{1}HNMR spectra of copolymers (PNI[illegible]-b-[illegible] (a), and enlargement one of them with label [illegible] detail (b). [illegible]lor figure can be viewed at wileyonlinelibrary.com]

similarly, "f" was quint[illegible]becaus[illegible] it was betw[illegible]een two methylene. The other hydrogen "g" [illegible]ue simi[illegible]r chemical shift and they all appeared at [illegible].19 p[illegible] showi[illegible]g a broad peak. By integrating every [illegible]eak, t[illegible] numbe[illegible] hydrogen can be drawn with the same pr[illegible]rti[illegible] the areas. Therefore, Nor-12C was obtained as expe[illegible].

Figure 2 shows the [illegible]netic of ROMP for Nor-12C and Nor-imid(Cl)-12C. The insert was ^{1}HNMR spectrum of mixture during polymerization reaction for monomer Nor-12C and corresponding polymers. By integrating the signal "a" at 6.14 ppm and peaks "a'" at 5.15–5.25 ppm, characteristic of the monomer olefin protons and the backbone double bond protons in polymer, conversion of ROMP polymerization could be calculated. In this study, different mixtures during different reacting times were characterized using ^{1}HNMR and the conversions of polymerization for monomer Nor-12C were obtained. The conversions of polymerization for monomer Nor-imid(Cl)-12C could also be calculated in the same way. The fitting curves a and b in Figure 2 were conversions versus polymerization time representing Nor-imid(Cl)-12C and Nor-12C, respectively. Basic data for conversion plots of polymerization has also been marked. It is clear that the polymerization for Nor-12C was so fast and finished completely after 60 s. However, the polymerization for Nor-imid(Cl)-12C was slower comparing with Nor-12C and went to completion until 20 minutes later. It is probably attributed to the molecular weight and stereo-hindrance effect of monomers. According to their activity, Nor-imid(Cl)-12C were mixed with Grubbs 3rd for polymerization prior to Nor-12C. The whole process of ROMP polymerization was conducted at room temperature. Five groups block copolymers were obtained according to the different feedings listed in Table I.

Figure 3(a) shows the ^{1}HNMR spectra of block copolymers PNICl$_m$-*b*-PNC$_n$. Compared with the ^{1}HNMR spectra for monomers in Figure 1, it is clear that the polymerization performed at room temperature went [illegible]pletion as indicated by the total disappearance of th[illegible] signal at [illegible]4 ppm, characteristic of the monomer olefin p[illegible]ns, and [illegible]e appearance of peaks at 5.15–5.25 ppm [illegible]of th[illegible] backbone double bond protons. Figure [illegible](b) sh[illegible]ws one [illegible] th[illegible]m as representative. The peaks of hydroge[illegible] [illegible]ifferen[illegible] chemical environments in both backbone and side [illegible]ins had all been labeled. Insert Figure 3(b) i[illegible]p[illegible]yl at 7.3[illegible] ppm in the end of polymer chain an[illegible] the [illegible]ble peaks at 5.15–5.25 ppm was for double bon[illegible] p[illegible]tons in p[illegible]mer backbone. The degree of polymerization (DP = m + n) f[illegible] block copolymer PNICl$_m$-*b*-PNC$_n$ could [illegible] obtained [illegible]sing end-group calculation method by integrating [illegible]m. The br[illegible]d peak at 8.29–8.10 ppm was for "i" in imidazoli[illegible]hich existed only in PNICl blocks, and the double peaks [illegible]t 5.15–5.25 ppm was from both PNICl and PNC blocks. By [illegible]ating them, the values for m and n can be calculated. The DP of five groups block copolymers were all calculated in the same way and they were same with theoretical feed at the beginning.

Magnetic block copolymers PNIFe$_m$-*b*-PNC$_n$ were prepared through post-modification with $FeCl_3 \cdot 6H_2O$. Due to the magnetic property of $FeCl_4^-$ anion, the magnetic polymers could

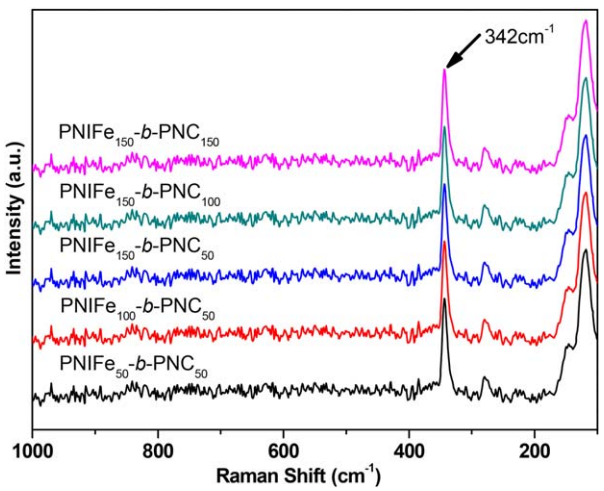

Figure 4. Raman spectra of magnetic block copolymers (PNIFe$_m$-b-PNC$_n$) with the $\lambda = 780$ nm. [Color figure can be viewed at wileyonlinelibrary.com]

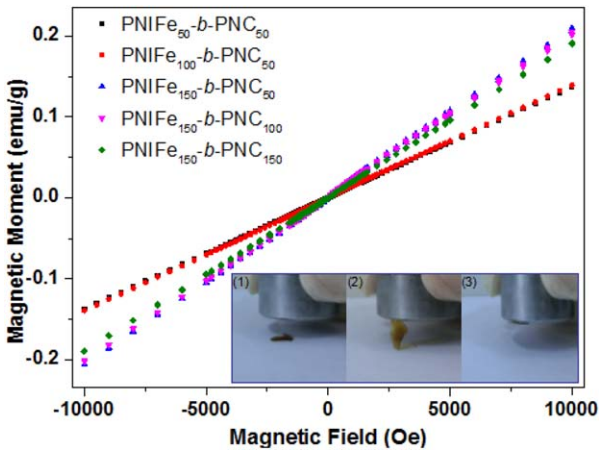

Figure 5. SQUID of magnetic block copolymers PNIFe$_m$-b-PNC$_n$ under room temperature (the inert is magnetic response of copolymer film PNIFe$_{150}$-b-PNC$_{50}$ to a neodymium magnet). [Color figure can be viewed at wileyonlinelibrary.com]

not be characterized by ^{1}H-NMR. According to Ref. 38, Raman spectrometer at 300 K was used to examine the presence of $FeCl_4^-$ anion in the magnetic polymers. Those peaks at 342 cm^{-1} in Figure 4 were reported and assigned very well to the symmetric Cl—Fe—Cl bond stretch vibrations of $FeCl_4^-$. It indicated that ferric chloride was combined into the magnetic polymers.

Magnetic Properties of Block Copolymers (PNIFe$_m$-*b*-PN)

In order to study the magnetic property of block copoly superconducting quantum interference device (SQUID) was used. For the measurements, a small amount polymers were located in a gelatin capsule and its m etic moment w s measured in the magnetic field range of −1 0 0 Oe when 300K. In Figure 5, all of the block copol rs showed a linear response to the magnetic fie which is typ for para-magnetic materials. The magnet susc bility can be calculated from the gradients of the magnetic fi dependence. From this graph, the magn susc ptibility w s determined with 13.76 × 10^{-6}, 13.98 × 1 6, 20.96 × 10^{-6}, 20.54 × 10^{-6}, and 19.04 × 10^{-6} e for ma tic b ck copolymers PNIFe$_{50}$-*b*-PNC$_{50}$, PN e$_{100}$-*b* NC$_{50}$, Fe$_{150}$-*b*-PNC$_{50}$, PNIFe$_{150}$-*b*-PNC$_{100}$, and NC$_{150}$, respectively. For PNIFe$_{50}$-*b*-PNC$_{50}$, PNIFe$_{100}$ NC$_{50}$, and PNIFe$_{150}$-*b*-PNC$_{50}$, the susceptibility increased with increase content of imidazolium $FeCl_4^-$ block in polymer chains. In general, the magnetic properties of polymers were determined by magnetic anion $FeCl_4^-$, so magnetic susceptibility increased when the content of $FeCl_4^-$ increased. As well, when the block of imdazolium $FeCl_4^-$ was constant, the increasing amount of alkyl substituted norbornene led to lower magnetic susceptibility compared with PNIFe$_{150}$-*b*-PNC$_{50}$, PNIFe$_{150}$-*b*-PNC$_{100}$, and PNIFe$_{150}$-*b*-PNC$_{150}$. However, it could be found that the magnetic susceptibility of PNIFe$_{150}$-*b*-PNC$_{150}$ was higher than that of PNIFe$_{50}$-*b*-PNC$_{50}$. It indicated that, when the percentage of imidazolium $FeCl_4^-$ was changeless, the magnetic properties could be enhanced by increasing the molecular weight of copolymers. This is probably due to that the polymers, with higher molecular weight, had a longer polymer chain which allowed magnetic units interact with each other around. As a result, the magnetic unit imidazolium $FeCl_4^-$ had an optimal order in the side-chain which led to higher magnetic susceptibility value under an applied external magnetic field. The insert (1), (2), (3) in Figure 5 show the response of a polymer film of PNIFe$_{150}$-*b*-PNC$_{50}$ to a neodymium magnet. The film showed good magnetic response to the magnetic field and eventually stuck on the magnet if close enough. Similar behavior was observed for all the other magnetic block polymer films.

Thermal Behaviors of the Magnetic Block Copolymers

The magnetic block copolymers PNIFe-*b*-PNC had a better thermal property like the other poly/(ionic liquid)s[38] as shown in Figure 6. Their qualities remained unchanged until being heated to above 350 °C. When the erature was above 1000 °C, they completely deg ed. The residual were in dark black and were probable i oxides, w ch had not been further studied in depth.

Morphology of the Co lym Films

As indicated fr Figu changing the contents of Nor-12C and Nor-im FeCl$_4^-$)−12 vo d have an influence on the magnetic prope s of copol ers. The magnetic properties of copol ers came m Nor-imid($FeCl_4^-$)−12C. Nor-12C was b ought in for imp ing the toughness of copolymer films, hich allowed the films to apply in wider fields. In addition, differences in hydrophilicity and chemical polarity for alkyl a midaz um $FeCl_4^-$ drove the copolymers self-assemble in appropriate conditions. In this study, the copolymer films were ed through spin coating method and three representatively copolymer films, PNIFe$_{50}$-*b*-PNC$_{50}$, PNIFe$_{150}$-*b*-PNC$_{50}$, and PNIFe$_{150}$-*b*-PNC$_{150}$, were studied for antimicrobial purpose. As the surface morphology has a significant effect on the antimicrobial activity, topographic structures of the copolymer films were further probed using AFM and SEM. The surface topography of magnetic copolymer films was witnessed by AFM and shown in Figure 7. The surface morphology showed different level of phase separation with the alterative content of Nor-12C and Nor-imid(Cl)-12C blocks. The roughness of film surface

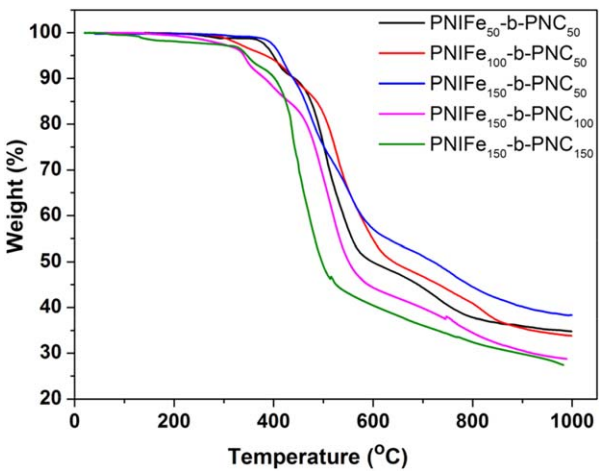

Figure 6. TGA curves of magnetic block copolymers under N_2 protection. [Color figure can be viewed at wileyonlinelibrary.com]

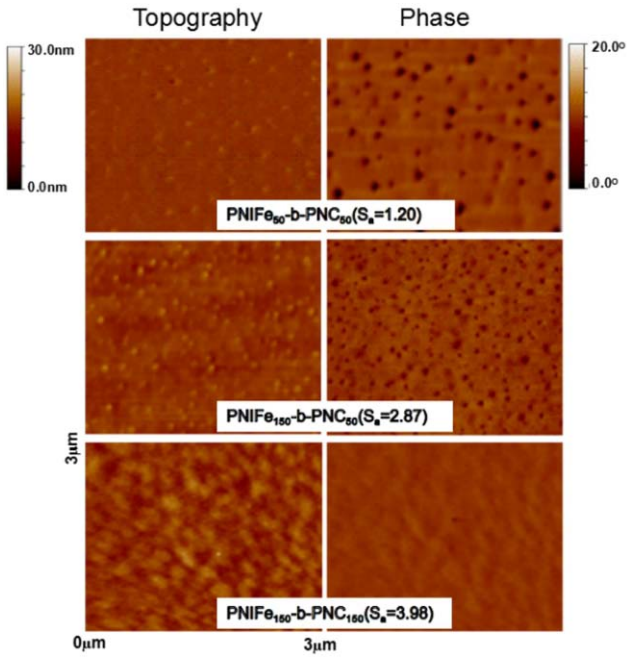

Figure 7. AFM topography and phase images of magnetic block copolymer films over a scope of 3 μm × 3 μm. [Color figure can be viewed at wileyonlinelibrary.com]

was shown as S_a, which varied from 1.20 to 3.98 nm. In the magnetic copolymers, it was the incompatibility between PNC and PIFe blocks that led to phase separation. During the p[illegible] of copolymer films under acetonitrile vapor pressure, the P[illegible] block was dissolved and migrated to the surface, which a[illegible] the morphology. For $PNIFe_{50}$-*b*-PNC_{50} and P[illegible]-*b*-PNC_{50}, increased content of imidazolium $FeCl_4^-$ led to more "bump" on the surface and the diameter of round domains in both topography and phase images became smaller. It is due to that acetonitrile was good solvent for quaternary imidazolium $FeCl_4^-$, increased content of PNIFe block resulted in more soluble chain segments and their precipitated in the surface. However, for $PNIFe_{150}$-*b*-PNC_{150}, increased content of both blocks generated for roughest surface due to the migration of PNIFe was restricted both by the high degree of polymerization of copolymers and the increased PNC content.

Furthermore, the similar phenomenon was shown in the SEM images of copolymer films (Figure 8). The complex interactions among various parameters resulted in the difference in the surface morphology, such as solvent, temperature of annealing, and content ratio of different blocks. The to[illegible]aphy and roughness resulted from the difference b[illegible]ween mig[illegible]ion rates of each segment to the surface in the a[illegible]g proces[illegible] Both of intermolecular ionic interactions of imida[illegible]m sal[illegible] groups and intramolecular actions b[illegible]ween alkyl s[illegible] chains and positively charged groups in im[illegible]zolium may provide thermodynamic driving force for micro-p[illegible]e separation, which is an assumption in other reports.[39–41] Besides, the special heterogeneous morphology on magnetic block copolymer film surface generated from phase separation may affect antimicrobial activity.

Antimicrobial Activity of the Magnetic Block Copolymer Films

The antimicrobial properties of the magnetic copolymer films were investigated via visual observation. Figure 9 shows the results obtained from the agar plating method. Transparent inhibition zones around each sample indicated that all the magnetic copolymer films had antimicrobial activity to *B. subtilis*

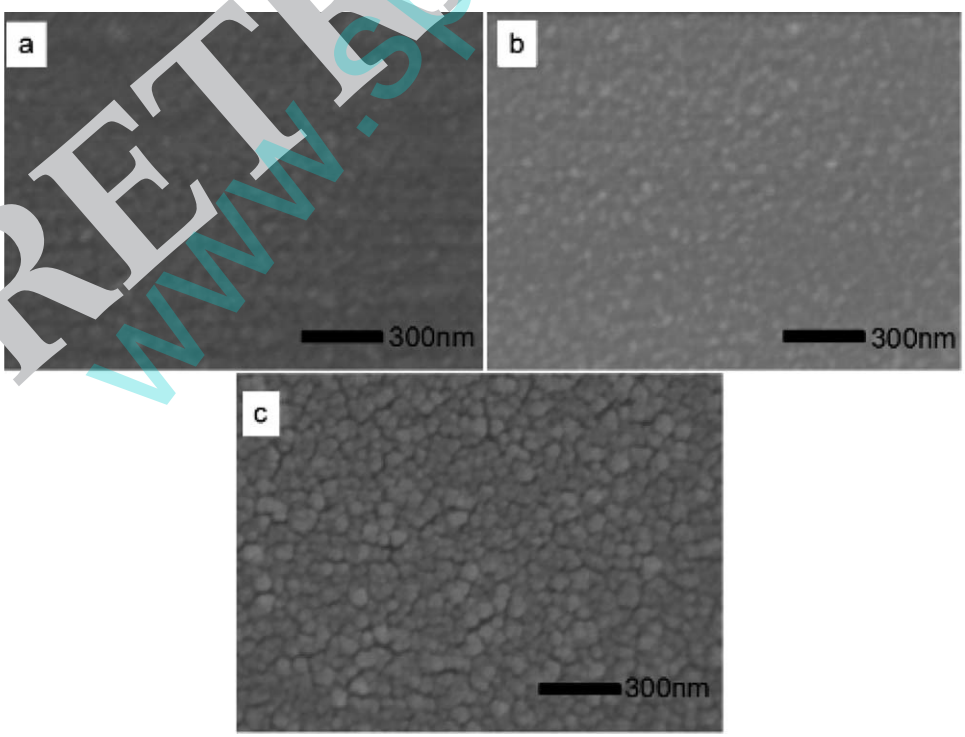

Figure 8. SEM images of magnetic block copolymer films: (a) $PNIFe_{50}$-b-PNC_{50}, (b) $PNIFe_{150}$-b-PNC_{50}, and (c) $PNIFe_{150}$-b-PNC_{150}.

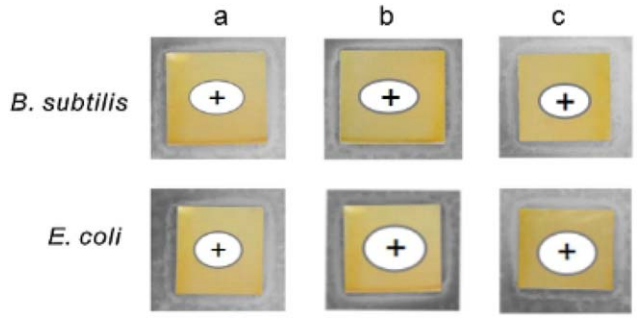

Figure 9. Antimicrobial activity of the magnetic block copolymer films: (a) $PNIFe_{50}$-b-PNC_{50}, (b) $PNIFe_{150}$-b-PNC_{50}, and (c) $PNIFe_{150}$-b-PNC_{150}. [Color figure can be viewed at wileyonlinelibrary.com]

and *E. coli*. Previous results had shown that quaternary ammonium salt tended to be more effective toward Gram-positive bacteria than Gram-negative bacteria.[27,42] This is due to that negative bacterium is wrapped with two kinds of cell membranes, while Gram-positive bacterium has only a single thin cell membrane, which is easily subject to be attacked by quaternary ammonium salt groups. However, the magnetic block copolymers based on imidazolium $FeCl_4^-$ had nearly antibacterial activity to both *B. subtilis* and *E. coli*. Consequently, they showed higher and broader-spectrum antimicrobial activity compared with other samples. In Figure 9, surface morphology seemingly exhibits no straightforward relationship with the antimicrobial properties, but the prominent effect on microorganism adhesion behaviors has been noticed.[43–45] Compared the surface roughness and topography of the block copolymers, the film of $PNIFe_{150}$-*b*-PNC_{150} had the largest roughness value ($S_a = 3.98$ nm). The imidazolium $FeCl_4^-$ groups on the heterogeneous surface could sufficiently interfere with bacteria by the increased contact area, resulting in more excellent antimicrobial activity. Therefore, with regard to structure–antimicrobial relationships, the surfaces with heterogeneous and rough surface morphology are expected to present better antimicrobial activity. The investigation on magnetic properties of magnetic films and their antimicrobial purpose is expected to promote further research on multifunctional materials.

CONCLUSIONS

A series of magnetic block copolymers PNIFe-*b*-PNC with a well-defined and controllable structure were prepared via ROMP polymerization and post modification. The magnetic copolymers showed high thermal stability and started to decompose around 350 °C. All of them had not much difference as the content of two blocks changed. Their magnetic properties were also characterized and all of them showed macroscopic magnetic response to magnet. The magnetic block polymers showed paramagnetic properties and their susceptibility were affected by the content of imidazolium $FeCl_4^-$ and the degree of polymerization of copolymers. The surface morphology of magnetic copolymer films and their antimicrobial activity for Gram-positive bacteria and Gram-negative bacteria were studied. In brief, the well-defined magnetic copolymers could show higher and broader-spectrum antimicrobial activity, which allowed further investigations for magnetic polymers based imidazolium $FeCl_4^-$ and expected to prepare multifunctional materials for wider application.

ACKNOWLEDGMENTS

This research was financially supported by the National Natural Science Foundation of China (no. 51375332), the Natural Science Foundation of Tianjin (no. 12JCYBJ12300) and the Specialized Research Fund for the Doctoral Program of Higher Education (no. 20120032110031).

REFERENCES

1. Sakal, S. A.; Lu, Y.; Jiang, X.; Shen, C.; Li, C. *J. Chem. Eng. Data* **2014**, *59*, 533.
2. Sun, M.; Zhang, H. Y.; Li B.; Liu, Y. *Macromolecules* **2013**, *46*, 4268.
3. Fujii, S.; Hamasaki, H.; Abe, H. Kuman ka, S.; Ohtaka, A.; Nakamura, E.; N mura Y. *J. Mater. Chem. A* **2013**, *1*, 4427.
4. Bilalis, P. Chaatzipavlo A.; Tziveleka, L. A.; Boukos, N.; Kord , G. *Mater. Chem.* **2012**, *22*, 13451.
5. C lliani, M.; nez-Segura, J.; Ruiz-Molina, D.; Massi, M.; Albonetti, C.; K a, C.; Veciana, J.; Biscarini, F. *Angew. Chem. Int. Ed.* **2005**, *44*, 888.
6. He, L.; W ng, M.; Ge, J.; Yin, Y. *Acc. Chem. Res.* **2012**, *45*, 31.
7. Korshak, Y. V.; Medvedeva, T. V.; Ovchinnikov, A. A.; pector, V. N. *Nature* **1987**, *326*, 370.
8. Rajca, A. *Chem. Rev.* **1994**, *94*, 871.
9. Hayashi, S.; Hamaguchi, H. *Chem. Lett.* **2004**, *33*, 1590.
10. Brown, P.; Bushmelev, A.; Butts, C. P.; Cheng, J.; Eastoe, J.; Grillo, I.; Heenan, R. K.; Schmidt, A. M. *Angew. Chem. Int. Ed.* **2012**, *51*, 2414.
11. Brown, P.; Butts, C. P.; Cheng, J.; Eastoe, J.; Russell, C. A.; Smith, G. N. *Soft Matter* **2012**, *8*, 7545.
12. Doebbelin, M.; Jovanovski, V.; Llarena, I.; Marfil, L. J. C.; Cabanero, G.; Rodriguez, J.; Mecerreyes, D. *Polym. Chem.* **2011**, *2*, 1275.
13. Jian, C.; Shaobei, Y.; Jinfang, Z.; Shuai, Z.; Yehai, Y. *RSC Adv.* **2012**, *2*, 12224.
14. Carrasco, P. M.; Tzounis, L.; Mompean, F. J.; Strati, K.; Georgopanos, P.; Garcia-Hernandez, M.; Stamm, M.; Cabañero, G.; Odriozola, I.; Avgeropoulos, A.; Garcia, I. *Macromolecules* **2013**, *46*, 1860.
15. Christopher, W. B.; Grubbs, R. H. *Prog. Polym. Sci.* **2007**, *32*, 1.
16. Leitgeb, A.; Wappel, J.; Christian, S. *Polymer* **2010**, *51*, 2927.
17. Colak, S.; Tew, G. N. *Macromolecules* **2008**, *41*, 8436.
18. Mitra, S.; Tang, G. C. *Polymer* **2015**, *63*, A1.
19. Zhang, Q.; Liu, H.; Chen, X.; Zhan, X.; Chen, F. *J. Appl. Polym. Sci.* **2010**, *132*, 41725.
20. Liu, W.; Wang, C. H.; Sun, J. F.; Hou, G. G.; Wang, Y. P.; Qu, R. J. *Chem. Biol. Drug. Des.* **2015**, *85*, 91.

21. Yao, D. D.; Guo, Y. J.; Chen, S. G.; Tang, J. N.; Chen, Y. M. *Polymer* **2013**, *54*, 3485.
22. Xu, F. J.; Li, H. Z.; Li, J.; Zhang, Z. X.; Kang, E.; Neoh, K. *Biomaterials* **2008**, *29*, 3023.
23. Fang, H. X.; Zhou, S. X.; Wu, L. M. *Appl. Surf. Sci.* **2006**, *253*, 2978.
24. Ngo, T. C.; Kalinova, R.; Cossement, D.; Hennebert, E.; Mincheva, R.; Snyders, R.; Flammang, P.; Dubois, P.; Lazzaroni, R.; Leclère, P. *Langmuir* **2014**, *30*, 358.
25. Paslay, L. C.; Abel, B. A.; Brown, T. D.; Koul, V.; Choudhary, V.; McCormick, C. L.; Morgan, S. E. *Biomacromolecules* **2012**, *13*, 2472.
26. Zhao, Y. F.; Zhu, L. P.; Jiang, J. H.; Yi, Z.; Zhu, B. K.; Xu, Y. Y. *Ind. Eng. Chem. Res.* **2014**, *53*, 13952.
27. Zhou, F.; Qin, X.; Li, Y.; Ren, L.; Zhao, Y.; Yuan, X. *Appl. Surf. Sci.* **2015**, *347*, 231.
28. Wiesenauer, E. F.; Edwards, J. P.; Scalfani, V. F.; Bailey, T. S.; Gin, D. L. *Macromolecules* **2011**, *44*, 5075.
29. Pulamagatta, B.; Pankaj, S.; Beiner, M.; Binder, W. H. *Macromolecules* **2011**, *44*, 958.
30. Yu, X.; Yuan, X.; Zhao, Y.; Ren, L. *RSC Adv.* **2015**, *5*, 92207.
31. Zoha, M.; Badri, A. L.; Raghavendra, R.; Zha, M. Y.; Hitesh, D.; Dobriyal, T.; Shunmugam, P. R.; Russell, T. P.; Tew, G. N. *Nat. Commun.* **2011**, *7*, 1.
32. Zha, Y.; Thaker, H. D.; Maddikeri, R. R.; Gido, S. P.; Tuominen, M. T.; Tew, G. N. *J. Am. Chem. Soc.* **2012**, *134*, 14534.
33. Sanford, M. S.; Love, J. A.; Grubbs, R. H. *Organometallics* **2001**, *20*, 5314.
34. Kugela, A.; Stafslien, S.; Chisholm, B. J. *Prog. Org. Coat.* **2011**, *72*, 222.
35. Liu, Y. W.; Leng, C.; Chisholm, B.; Stafslien, S.; Majumdar, P.; Chen, Z. *Langmuir* **2013**, *29*, 2897.
36. Majumdar, P.; Lee, E.; Gubbins, N.; Stafslien, S. J.; Daniels, J.; Thorson, C. J.; Chisholm, B. J. *Polymer* **2009**, *50*, 1124.
37. Majumdar, P.; He, J.; Lee, E.; Kallam, A.; Gubbins, N.; Stafslien, S. J.; Daniels, J.; Chisholm, B. J. *J. Coat. Technol. Res.* **2010**, *7*, 455.
38. Zhou, C.; Yu, X.; Ma, H.; Huang, X.; Zhang, H.; Jin, J. *Carbohydr. Polym.* **2014**, *105*, 300.
39. Liu, G.; Wu, G.; Jin, C.; Kong, Z. *Prog. Org. Coat.* **2015**, *80*, 150.
40. Zhang, A.; Liu, Q.; Lei, [illegible]; [illegible]ong, S.; [illegible] Y. *React. Funct. Polym.* **2015**, *88*, 39.
41. Farah, S.; Aviv, O.; [illegible]aout, N.; Ra[illegible] S.; Beyth, N.; Dom, A. J. *Colloids Surf. B. [illegible]int[illegible]ces* **201[illegible]** *128*, 608.
42. Qin, X.; Li, Y.; Zhou[illegible] Ren, [illegible]; Zhao, Y.; Yuan, X. *Appl. Surf. Sci.* [illegible]**5**, *328*, 185.
43. Hsu, [illegible] C.; [illegible], J.; Bo[illegible]ca-Tasciuc, D. A.; Worobo, R. W.; [illegible]u, C. I. *Appl. Environ. Microbiol.* **2013**, *79*, 2703.
44. Mitik-DinevaWa[illegible], N. J.; Mocanasu, R. C.; Stoddart, P. R.; Crawford, [illegible]. J.; Ivanova, E. P. *Biotechnol. J.* **2008**, *3*, 536.
45. [illegible]uckett, [illegible]. D.; Lee, P. P.; Ciombor, D. M.; Aaron, R. K.; [illegible], T. J. *Acta Biomater.* **2010**, *6*, 2352.